Gelled polymerizable microemulsions. Part 3 Rheology†‡

Miguel Magno,*[a] Renate Tessendorf,[ab] Bruno Medronho,[c] Maria G. Miguel[c] and Cosima Stubenrauch[ad]

Received 16th July 2009, Accepted 27th August 2009
First published as an Advance Article on the web 24th September 2009
DOI: 10.1039/b914281a

This is the first report on the rheological properties of oil-gelled polymerizable bicontinuous microemulsions. The polymerizable base system consists of H_2O/NIPAm/BisAm – *n*-dodecane – $C_{13/15}E_5$ (a technical grade *n*-alkyl polyglycol ether), where NIPAm denotes the monomer *N*-isopropylacrylamide and BisAm the cross-linker *N*,*N*′-methylene bisacrylamide. For the planned polymerization of the aqueous phase a scaffold is needed to preserve the structure of the templating microemulsion during the polymerization. This scaffold is supposed to be a gel, which was formed by adding the gelator 12-hydroxyoctadecanoic acid (12-HOA) to the oil phase of the microemulsion. The influence of the water-to-oil ratio α, of the gelator concentration β, and of the monomer concentration ψ on the rheological behavior of gelled microemulsions has been studied in detail. The most important result of the study at hand is the observation of a transition from a high viscous solution to a gel, *i.e.* from a transient to a permanent network, with increasing gelator concentration and increasing amount of the oil phase. In other words, it is only under well-defined conditions that an oil-gelled microemulsion is formed.

1. Introduction

Microemulsions as templates for nanostructured materials have been of great interest for a long time. These complex fluids, which contain water, oil and surfactant, are thermodynamically stable and can appear as discrete particles of one phase dispersed in the second (water droplets in oil or *vice versa*) or as a bicontinuous structure consisting of two equal subphases, namely oil and water.[1] Using bicontinuous microemulsions as templates should lead to a material with a high surface area and a structure equal to the structure of the template. A promising application could be the use of microemulsions as templates for polymers of various nanostructures. However practical problems are related to the high flexibility of the surfactant monolayer and to the different time scales of structural changes in a microemulsion (~1 μs) compared to the kinetics of polymerization (~1 ms per step).

A polymerizable bicontinuous microemulsion system with a gelled oil phase has been developed previously in our group to arrest structural changes during the polymerization.[2,3] The chosen system consists of the ternary base system water – *n*-dodecane – $C_{13/15}E_5$ (a technical grade *n*-alkyl polyglycol ether). The gelator for the oil phase was 12-hydroxyoctadecanoic acid (12-HOA), and the polymerizable aqueous phase contained the monomer *N*-isopropylacrylamide (NIPAm) and the cross-linker *N*,*N*′-methylene bisacrylamide (BisAm). Phase diagrams were studied in detail to elucidate the effect of each of the components on the phase behavior of the microemulsion. These studies allowed for the determination of the conditions under which a clear, gelled phase, located in the one-phase region of a H_2O/NIPAm/BisAm – *n*-dodecane/12-HOA – $C_{13/15}E_5$ microemulsion, is formed.[2] The structure of the gelled microemulsion was studied *via* conductivity, small angle neutron scattering (SANS), and NMR self-diffusion measurements.[3] It has been proven that gelling a bicontinuous microemulsion does not change the structure of the microemulsion—it is still bicontinuous with the same domain sizes as the non-gelled counterpart. However, the structure of the gel network in the gelled microemulsion has not been determined yet. We assume that it resembles the structure of the respective binary gel, which consists of long thin crystalline fibrils that are connected *via* crystalline nodes.[4] To verify this assumption the thickness and the shape of the gel fibrils as well as the distance between the nodes needs to be determined. SANS and transmission electron microscopy (TEM) measurements are currently under way to complete the structural characterization of the gelled microemulsion.

The current study expands on that of our previous work[2,3] and aims at investigating the rheological properties of gelled bicontinuous microemulsions. Note that the present study is the first of its kind. The questions we wanted to answer are: Are the high-viscous microemulsions which we observed in our previous work indeed gels or only high viscous solutions? Under which condition is a microemulsion a gel in the first place? Is there a difference between a gelled microemulsion and the respective binary organogel from a rheological point of view? How is the rheological behavior of a gelled microemulsion influenced if one changes the water-to-oil ratio α, the gelator concentration β, and the monomer concentration ψ?

[a]*School of Chemical and Bioprocess Engineering, Centre for Synthesis and Chemical Biology (CSCB), SFI-Strategic Research Cluster in Solar Energy Conversion, University College Dublin, Belfield, Dublin, 4, Ireland. E-mail: luis.magno@ucd.ie; Fax: +353-1-716-1177; Tel: +353-1-716-1691*
[b]*Institut für Festkörperforschung, Forschungszentrum Jülich, Leo-Brandt-Strasse, D-52425 Jülich, Germany*
[c]*Department of Chemistry, University of Coimbra, Rua Larga, Coimbra 3004-535, Portugal*
[d]*Institut für Physikalische Chemie, Universität Stuttgart, Pfaffenwaldring 55, 70569 Stuttgart, Germany*

† Electronic supplementary information (ESI) available: Fig. S1–S3 and Table S1. See DOI: 10.1039/b914281a

‡ For parts 1 and 2 see ref. 2 and 3, respectively.

2. Experimental part

2.1. Materials

The gelator 12-HOA, the monomer NIPAm, and the cross-linker BisAm were purchased from Acros Organics. According to the manufacturer, these chemicals have a purity of 99%. The gelator, 12-HOA was used as received and NIPAm was recrystallized twice from *n*-hexane. The technical grade surfactant Lutensol® AO5 (nonionic *n*-alkyl polyglycol ether with an average molecular structure of $C_{13/15}E_5$) was donated by BASF and used as received. *n*-Dodecane (purity of 99%) was purchased from Sigma-Aldrich. The water was purified by a Milli-Q system or alternatively doubly distilled.

2.2. Phase diagrams

2.2.1. Microemulsions. The experimental procedure to determine phase diagrams of gelled microemulsions is explained in ref 2. Of importance for the present study are the definitions to characterize the samples. The masses of the individual components water (A), oil (B), surfactant (C), monomer (NIPAm), cross-linker (BisAm), and gelator (12-HOA) are denoted m(A), m(B), m(C), m(NIPAm), m(BisAm), and m(12-HOA), respectively. The composition of the samples is given in mass fractions. It holds for the mass fraction of oil in the water plus oil mixture

$$\alpha = \frac{m(\mathrm{B})}{m(\mathrm{A}) + m(\mathrm{B})} \tag{1}$$

for the overall mass fraction of the surfactant in the sample

$$\gamma = \frac{m(\mathrm{C})}{m(\mathrm{total})} \tag{2}$$

for the mass fraction of NIPAm + BisAm in the aqueous phase

$$\psi = \frac{m(\mathrm{NIPAm}) + m(\mathrm{BisAm})}{m(\mathrm{A}) + m(\mathrm{NIPAm}) + m(\mathrm{BisAm})} \tag{3}$$

and for the mass fraction of 12-HOA in the oil phase

$$\beta = \frac{m(\text{12-HOA})}{m(\mathrm{B}) + m(\text{12-HOA})} \tag{4}$$

Various amounts of the components were weighed into test tubes (containing a magnetic stirring bar) which were sealed with polyethylene stoppers. All phase diagrams were determined at a fixed water-to-oil ratio α as a function of the temperature T and the total surfactant concentration γ. The focus was on the location of the 1-phase region of the microemulsion for which the lower ($\underline{2} \rightarrow 1$) and the upper phase boundary ($1 \rightarrow \bar{2}$) were measured (see ref. 2 for details). Microemulsion gelation was achieved with different amounts of gelator, which were added to the oil phase. All sample compositions, the phase transition temperatures T_{min} ($\underline{2} \rightarrow 1$) and T_{max} ($1 \rightarrow \bar{2}$), the middle temperatures $T_{\mathrm{middle}} = (T_{\mathrm{min}} + T_{\mathrm{max}})/2$, and the temperatures at which the measurements were carried out are listed in Table 1.

Note that in the case of technical grade surfactants the phase boundaries usually shift to higher or lower temperatures if a new batch is taken as each batch differs slightly in composition. As the surfactants used for the rheological measurements and for the phase studies were from different batches, the phase boundaries of the samples used for rheometry were re-measured. Thus the phase boundaries listed in Table 1 and those shown in the phase diagrams sometimes differ by 1–2 °C. In the present study the rheological measurements were always carried out as close as possible to T_{middle} of the actual sample.

2.2.2. Binary organogels. Various binary mixtures consisting of the gelator 12-HOA and *n*-dodecane were weighed into test tubes which contained a magnetic stirring bar and were sealed with polyethylene stoppers. The sol–gel transition temperatures of all samples were determined in a water bath with a precision of ±1 °C. The rheological measurements were carried out with samples that contained 1, 2, and 3 wt% 12-HOA ($\beta = 0.01, 0.02, 0.03$).

2.3. Rheometry

The gel-like rheological properties can be qualitatively studied by simple experimental tests without using a rheometer. These are known as "tabletop" tests and are based on visual observation, which are particularly useful in determining the sol–gel transition boundary.[5] For the "tabletop" experiments samples were placed in a water bath at the desired temperature. The physical state (sol or gel) was checked by tube inversion at different temperatures.

For a more precise and quantitative analysis rheological measurements were performed on a Reologica Stress rheometer equipped with an automatic gap setting. The viscoelastic properties of the system were studied by dynamic oscillatory experiments, which provide information on the linear viscoelastic behavior of materials through the determination of the complex shear modulus[6]

$$G^*(\nu) = G'(\nu) + i\, G''(\nu) \tag{5}$$

where G' is the storage and G'' the loss modulus. The temperature was regulated by a circulating water bath with an accuracy of ±0.3 °C. A metallic plate–plate measuring system with a gap of 2 mm for the binary systems and of 0.5 mm for the microemulsions was used. Different gap sizes were used to optimize the experimental conditions (the gap size did not influence the results). Prior to any frequency-sweep measurement a stress-sweep measurement was performed for each sample at a constant frequency of 1 Hz to ensure that all tests were carried out in the linear viscoelastic regime. The stress was varied from 0.001 to 50 Pa and the lowest stress value of the linear regime was chosen for the frequency sweep measurements. The frequency-sweep experiments were carried out at a constant stress of 2 Pa for the binary organogels and the gelled microemulsions, respectively, and of 0.2 Pa for the non-gelled microemulsions. The frequency range was 0.1–10 Hz for the gelled microemulsions and 0.01–10 Hz for the non-gelled microemulsions and the binary organogels. Different frequency ranges were used in order to capture the main features (*i.e.* the crossing of G' and G'') of the different systems.

All microemulsion samples were heated up to 60 °C, homogenized *via* stirring, and then cooled down to 4 °C where they were kept for 1 h. Afterwards the gel was transferred to the plate and equilibrated for 30 min at the chosen experimental temperature (see Table 1). The binary system was studied at various temperatures, ranging from 25 to 80 °C in steps of 5 °C. Prior to

Table 1 Compositions and phase transition temperatures of the system H_2O/NIPAm/BisAm – *n*-dodecane/12-HOA – $C_{13/15}E_5$. The definitions of α, β, γ, and ψ are given in eqn (1)–(4). T_{min} is the lower and T_{max} the upper phase transition temperature for the given composition, $T_{middle} = (T_{min} + T_{max})/2$, and T_{exp} indicates the temperature at which the rheological measurements were carried out

Sample	α	β	γ	ψ	T_{min}	T_{max}	T_{middle}	T_{exp}
non-gelled base system								
I	0.50	0	0.120	0	45.92	48.92	47.42	47.0
β-variation (α = 0.5, ψ = 0.075)								
e	0.50	0.029	0.130	0.075	29.74	37.19	33.47	33.5
f	0.50	0.031	0.109	0.075	35.39	37.40	36.40	36.5
g	0.50	0.041	0.109	0.075	33.71	37.21	35.46	35.5
α-variation (β = 0.031, ψ = 0.075)								
f	0.50	0.031	0.109	0.075	35.39	37.40	36.40	36.5
b	0.34	0.031	0.099	0.075	30.89	35.35	33.12	33.0
c	0.30	0.031	0.083	0.075	32.23	34.72	33.48	34.0
d	0.25	0.031	0.069	0.075	31.91	34.40	33.16	33.0
α-variation (β = 0.041, ψ = 0.14)								
h	0.50	0.041	0.130	0.138	31.72	36.22	33.97	35.0
i	0.60	0.041	0.150	0.140	36.21	38.70	37.46	37.0
ψ-variation (α = 0.5, β = 0.041)								
g	0.50	0.041	0.109	0.075	33.71	37.21	35.46	35.5
h	0.50	0.041	0.130	0.138	31.72	36.22	33.97	35.0

any measurement at each new temperature, the sample was left to equilibrate for 30 min. For three of the gelled microemulsions (h, i, and j) temperature scans were carried out (see the ESI†) in steps of 1 °C (samples h and j) and 0.5 °C (sample i). During the temperature scans the samples were kept for 30 min at the respective temperature prior to the measurement.

3. Rheology of reference systems

3.1. Binary organogel 12-HOA – *n*-dodecane

"Tabletop" experiments were carried out to determine the sol–gel transition temperatures of the binary system 12-hydroxyoctadecanoic acid (12-HOA) and *n*-dodecane. 12-HOA is a well-known low molecular mass organic gelator (LMOG), which is capable of forming strong organogels with some solvents.[4,7–9] As the phase diagram of the binary system 12-HOA – *n*-dodecane has not been studied in detail yet, we determined the sol–gel transition temperatures T_g as a function of the gelator mass fraction β in order to have a reference for the discussion of the gelled microemulsions. The results are represented in Fig. 1.

As can be seen in Fig. 1, an increase of the gelator content from 0.5–4 wt% (β = 0.005–0.04) leads to an increase of the sol–gel transition temperature T_g from 45–65 °C. In order to check the reliability and accuracy of the tabletop experiments, additional dynamic oscillatory tests were carried out. In one set of measurements the frequency of the oscillations was kept constant at 1 Hz and the rheological parameters were measured as a function of the temperature, while in a second set the temperature was kept constant and the rheological parameters were measured as a function of the frequency. The dynamic data of selected samples are represented in Fig. 2.

In Fig. 2 (left) the storage modulus G' obtained at 1 Hz is plotted as a function of the temperature for three selected β values. Two things are worth mentioning. Firstly, at low temperatures an increase of β leads to an increase of the elastic properties, *i.e.* of G'. The storage modulus increases by nearly one order of magnitude if one increases the gelator concentration from 1 to 3 wt%. Secondly, an increase of the temperature

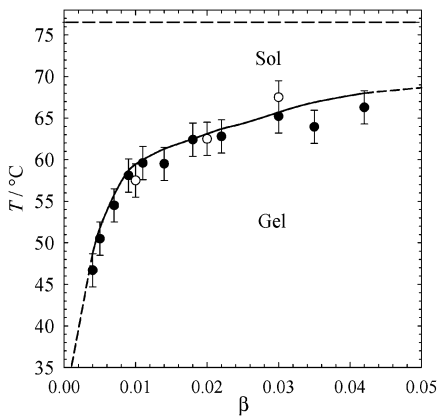

Fig. 1 Sol–gel transition temperature T_g *versus* gelator mass fraction β of the binary system *n*-dodecane – 12-HOA. Open symbols represent the results of dynamic oscillatory measurements at 1 Hz (see Fig. 2, left), while full symbols correspond to the results obtained *via* the "tabletop" method (data are taken from ref. 2). The horizontal dashed line represents the melting temperature of pure solid 12-HOA.

eventually leads to an abrupt decrease of the storage modulus for all three samples. The temperature (or rather the temperature range) at which the G' values drops by more than 4 orders of magnitude is higher the larger the gelator concentration β. In other words, the sol–gel transition boundary is shifted to higher temperatures with increasing β. The respective transition temperatures are included in Fig. 1 (open symbols) and a comparison between the oscillatory and the tabletop experiments shows that the latter are indeed an appropriate tool to measure sol–gel transition temperatures. In Fig. 2 (right) the storage modulus G' and the loss modulus G'' of the sample with β = 0.03 are plotted as a function of the frequency for two selected temperatures. A typical gel-like behavior is observed at the lower temperature (25 °C), where G' and G'' are frequency independent in the studied frequency range and G' is about 1 order of magnitude higher than G''. At the higher temperature (75 °C) both moduli are strongly frequency dependent and orders of magnitudes lower compared to the values measured at 25 °C.

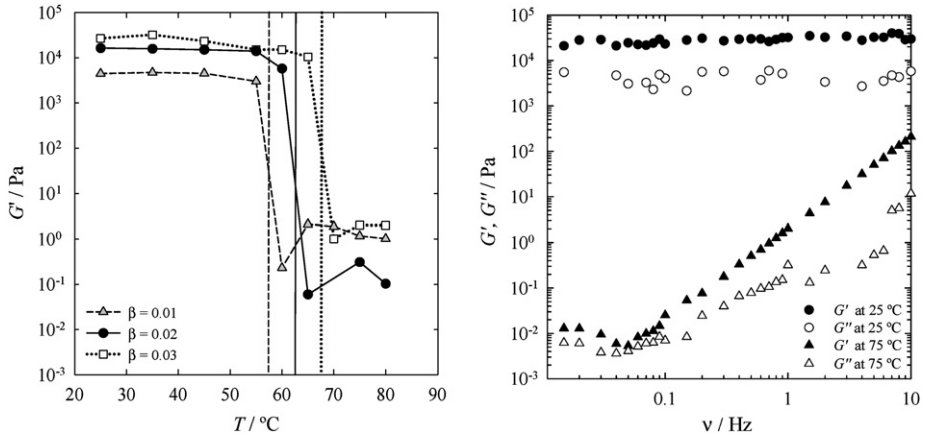

Fig. 2 (left) Storage modulus G' measured at 1 Hz as a function of the temperature T for three different weight fractions of 12-HOA in *n*-dodecane, namely $\beta = 0.01$, $\beta = 0.02$, and $\beta = 0.03$. The vertical lines indicate the temperatures at which G' abruptly changes, *i.e.* the sol–gel transition temperature T_g of the respective sample. (right) Storage modulus G' and loss modulus G'' as a function of the frequency for the sample with $\beta = 0.03$ measured below (25 °C) and above (75 °C) T_g.

Note that for a low viscous, unstructured sol one expects Newtonian behavior, which is obviously not the case. The observations that $G' > G''$ and that the values of G' and G'' are higher than expected for a Newtonian liquid indicate that the gel was not completely destroyed and that the sample still had some gel character. In any case, the significant difference of the rheological behavior at 25 °C and 75 °C are obvious and the data are in perfect agreement with those obtained by Terech *et al.*[8]

We would like to conclude this section by a short description of the gel structure, which is needed to understand the results obtained for the gelled microemulsions (see section 4). Binary 12-HOA organogels were found to consist of a rigid fibrillar network with rigid junction zones. Both the fibrils and the junctions are crystalline[4,8–10] and are generated *via* self-assembly of 12-HOA molecules, which is why the resulting gel network is called a self-assembled fibrillar network (SAFIN).[11] The dramatic decrease of G' upon reaching the sol–gel transition temperature reflects the loss of interconnectivity between the fibers, *i.e.* the melting of the crystalline 12-HOA network. Despite a lot of research activity it still is impossible to predict whether a gelator gels a given solvent and if it does what the properties and the structure of the resulting gel will be. For example, for 12-HOA gels it has been found that the structure of the gel network depends on the polarity of the solvent. More precisely the shape of the fibrillar cross-section was found to be rectangular for cyclohexane and dodecane, square for benzene and toluene (side ~20 nm), and round for nitrobenzene (diameter ~30 nm).[4,8] Thus the less polar the organic solvent is, the flatter the fibrils are—an explanation for this observation has not been found yet. The distance between the junctions is 1–2 orders of magnitude larger than the cross-sections of the fibrils and mainly depends on the total gelator concentration, *i.e.* the larger the gelator concentration the closer the junctions, which, in turn, strengthens the gel.

3.2. Non-gelled microemulsions

For comparison, oscillatory measurements were carried out with the non-gelled bicontinuous base microemulsion H_2O – *n*-dodecane – $C_{13/15}E_5$. As the phase diagram was determined in a previous study[2] only the phase boundaries of the freshly prepared sample needed to be re-measured (see explanation in section 2.2.1). The sample composition, the phase transition temperatures T_{min} ($\underline{2} \rightarrow 1$) and T_{max} ($1 \rightarrow \bar{2}$), the middle temperature $T_{middle} = (T_{min} + T_{max})/2$, and the temperature at which the measurements were carried out are also listed in Table 1, while the phase diagram (right) and the dynamic mechanical spectrum (left) are represented in Fig. 3.

In Fig. 3 (left) the dynamic moduli G', G'' and the complex viscosity η^* ($\eta^* = (G'^2 + G''^2)^{1/2}\,\omega^{-1}$) of the sample indicated in Fig. 3 (right) are presented. The non-gelled microemulsion exhibits a liquid-like behavior with the G' values being lower than the G''-values up to 0.1 Hz and $G' \sim G''$ above 0.1 Hz. Note that the moduli are very low (up to 8 orders of magnitude lower than the values obtained for the binary organogel) and thus subject to a significant error. In any case, G' is proportional to ω^2 while G'' scales with ω which is in agreement with a simple Maxwell model for linear viscoelastic behavior. Moreover, the complex viscosity is frequency independent. All these observations are in agreement with other bicontinuous microemulsions (reviewed in ref. 12).

A closer look on the structure of a bicontinuous microemulsion reveals that it consists of two interwoven sub-phases, which is why it is often called "sponge phase" or "plumbers nightmare" (latest reviews are in ref. 1 and 13). It is interesting to note that, despite being a multiple connected bilayer structure, the structural relaxation times of bicontinuous microemulsions are typically less than 1 ms (bilayers are fluid and passages can freely slide), while relaxation times of gels are a few hundred seconds.

4. Rheology of gelled microemulsions

As outlined in the introduction it was found that the microemulsion structure is not altered by gelling the oil subphase. However, the structure of the gel network, which causes the gelation of the whole microemulsion, still has to be determined. The interested reader is referred to ref. 3, where a suggestion for a possible structure is made. However, in this paper we will focus on the rheology of gelled bicontinuous microemulsions and discuss structure–property relations whenever reasonable.

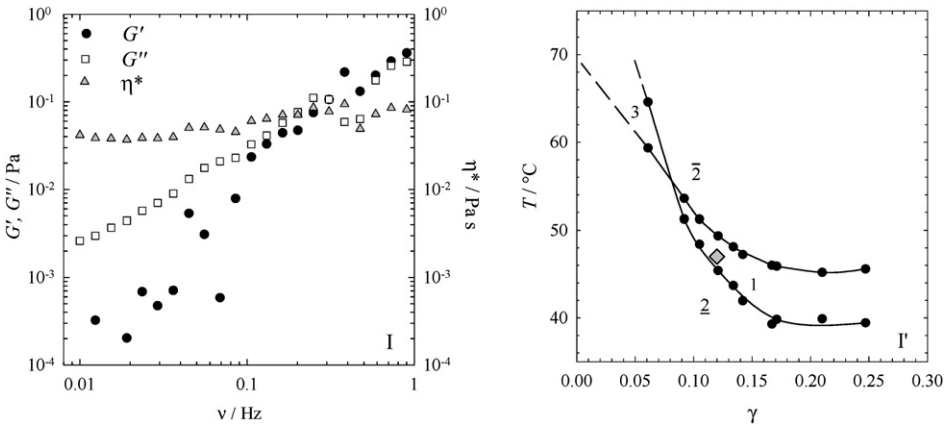

Fig. 3 Storage modulus G', loss modulus G'', and complex viscosity η^* as a function of the frequency ν (left) and phase diagram (right) of the system H_2O – *n*-dodecane – $C_{13/15}E_5$ at $\alpha = 0.5$. The diamond in the phase diagram represents the surfactant concentration γ and temperature T_{exp} of the sample used for the rheological measurements (see section 2.2.1 and Table 1). Data of phase diagram are adapted from ref. 2.

In our previous work, phase diagrams of the system H_2O/NIPAm/BisAm – *n*-dodecane/12-HOA – $C_{13/15}E_5$ were measured at a fixed water-to-oil ratio ($\alpha = 0.5$) and a fixed monomer concentration ($\psi = 0.075$) for different gelator concentrations β to find the conditions under which the microemulsion behaves like a gel.[2] It was found that at least 2.9 wt% of 12-HOA in the oil phase is required to have a sol–gel transition boundary that passes the 1-phase region of the microemulsion, while at 3.1 wt% of 12-HOA the whole 1-phase region was gelled. Thus the minimum gelator concentration in the oil phase required to gel the whole 1-phase region is 3.1 wt%. Note that in the previous work the sol–gel transition temperatures were only determined *via* "tabletop" measurements.

Being able to control the strength of the gel is of utmost importance for our work as the final goal is to polymerize the aqueous phase of the microemulsion, for which a scaffold as strong as possible is needed to preserve the structure during the polymerization. In order to quantify the strength of the gelled microemulsions and to find out under which conditions the strongest possible gel is formed, dynamic oscillatory measurements were performed. The influence of various parameters such as the gelator concentration β, (section 4.1), the water-to-oil ratio α, (section 4.2), the monomer concentration ψ, (section 4.3), the type of oil (ESI†), and the temperature (ESI†) were studied in detail. For all systems the respective phase diagrams had to be determined in order to specify the experimental temperatures and sample compositions. All rheological studies were carried out in the 1-phase region of the phase diagram at the lowest possible surfactant concentration γ as it is only in this region where a bicontinuous structure is formed. The compositions of all samples, the phase transition temperatures T_{min} ($\underline{2} \rightarrow 1$) and T_{max} ($1 \rightarrow \bar{2}$), the middle temperatures $T_{middle} = (T_{min} + T_{max})/2$, and the temperatures at which the measurements were carried out are listed in Table 1 and Table S1 (ESI†), while the rheological data and the phase diagrams are presented in Fig. 4–7, S1 (ESI†), and S3 (ESI†).

4.1. Influence of the gelator concentration β

Let us first consider the influence of the gelator mass fraction β on the viscoelastic properties of the H_2O/NIPAm/BisAm – *n*-dodecane/12-HOA – $C_{13/15}E_5$ microemulsion system at $\alpha = 0.5$ and $\psi = 0.075$. In Fig. 4 the dynamic rheological data (left) and the phase diagrams (right) for three β values are shown.

A look at the phase diagrams reveals that the sol–gel transition temperatures shift towards higher values with increasing gelator concentration as was the case for the binary organogel (see Fig. 1 and Fig. 2). What is different, however, are the absolute sol–gel transition temperatures. Comparing systems with similar β-values one sees that the sol–gel transition of the gelled microemulsions takes place at temperatures which are 20–30 °C lower compared to the binary organogel. We will come back to this below. Another important observation is the fact that an increase of the gelator concentration from 3.1 to 4.1 wt% has no significant affect on the position and extension of the 1-phase region of interest (*i.e.* the 1-phase region at low surfactant concentrations γ), while it strongly affects the position of the sol–gel transition boundary. In other words, the distance between the region of the gelled bicontinuous microemulsion and the sol–gel transition boundary increases, which, in turn, should be reflected in a stronger gel. Indeed, as is seen in Fig. 4 (left), the strength of the gel strongly increases with increasing gelator concentration. While at $\beta = 0.029$ a liquid-like (sol) character is observed up to 2 Hz, the samples with $\beta = 0.031$ and 0.041 clearly have a solid-like character. At the lowest β-value of 0.029 a transition from a liquid-like ($G' < G''$) to a solid-like ($G' \gg G''$) character is observed around 2 Hz. Thus the main relaxation time of the system is ~0.5 s, which is very fast for a viscoelastic system. The very small increase of β from 0.029 to 0.031 leads to a completely different picture. The elastic properties now clearly dominate the viscous properties and a system with an extremely long relaxation time is obtained in the linear viscoelastic regime. The same holds true for $\beta = 0.041$. However, the G' values of the system with the higher gelator concentration are 3–4 times and the G'' values are even 100 times higher than those of the system with $\beta = 0.031$. Due to this different increase of G' and G'' the ratio of G':G'' is 500:1 at $\beta = 0.031$ and 10:1 at $\beta = 0.041$. Comparing the results obtained for $\beta = 0.031$ with those obtained for the binary organogel at $\beta = 0.03$ (Fig. 2 (right)) one sees two differences. Firstly, the ratio of G':G'' is roughly 10:1 for the binary organogel (as is the case for the microemulsion with $\beta = 0.041$), while it is 500:1 for the gelled microemulsion. Secondly, the absolute G'

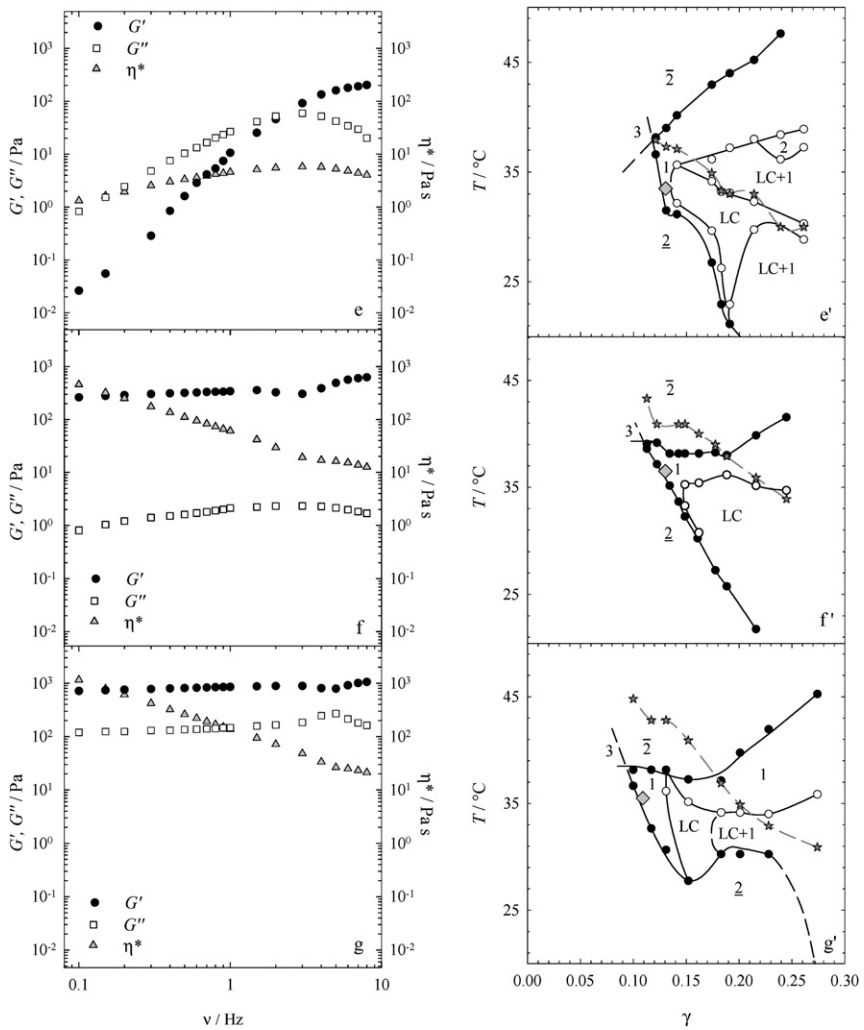

Fig. 4 Storage modulus G', loss modulus G'', and complex viscosity η^* as a function of the frequency ν (left) and phase diagrams (right) of the system H_2O/NIPAm/BisAm – *n*-dodecane/12-HOA – $C_{13/15}E_5$ at $\alpha = 0.5$ and $\psi = 0.075$ measured for three different gelator concentrations β, namely $\beta = 0.029$ (sample e), $\beta = 0.031$ (sample f), $\beta = 0.041$ (sample g). The stars in the phase diagrams represent the sol–gel transition temperatures T_g and the diamonds the surfactant concentration γ and temperature T_{exp} of the samples used for the rheological measurements (see section 2.2.1 and Table 1). Data of all phase diagrams are adapted from ref. 2.

values of the binary organogel are 50–100 times and the corresponding G'' values are nearly 4 orders of magnitude larger than those of the gelled microemulsion.

Summarizing the results obtained so far one can say that the strength of the gel increases with increasing gelator concentration for both the gelled microemulsion and the binary organogel. However, comparing the binary organogel with the gelled microemulsion at equal gelator concentrations one sees that the former is a much stronger gel, which is reflected in the higher sol–gel transition temperatures and the higher G' values. We can understand this finding in the following way. For the formation of a permanent network a minimum number of cross-links have to be present, which, in turn, depends on the total gelator concentration. In the case of the gelled microemulsions one has to keep in mind that the gelator concentrations refer to the oil phase only. What is gelled, however, is the total system. From a structural point of view there are two possibilities. The gel may only be formed in the oil phase and thus a closely cross-linked network is required to also "arrest" the non-gelled aqueous phase. Alternatively, the gel network may expand over the whole sample. In both cases, the presence of the aqueous phase renders the network inhomogeneous. Since inhomogeneous and coarse networks tend to be weaker (effectively, defects were introduced in the network) compared to well-structured gel networks, this explains why the gelled microemulsion is weaker than the binary organogel. Independent on what the structure would be the presence of the aqueous phase obviously dilutes and thus weakens the gel network. This "dilution" will be further studied in section 4.2, where we varied the water-to-oil ratio. Another possible reason for the reduced strength of the gelled microemulsion in comparison to the binary organogel is the surface-activity of the gelator. This means that parts of the gelator are adsorbed at the water–oil interface and are thus not available for network formation.[3] However, this effect is expected to play a minor role compared to the structural changes which are induced by the presence of the aqueous phase.

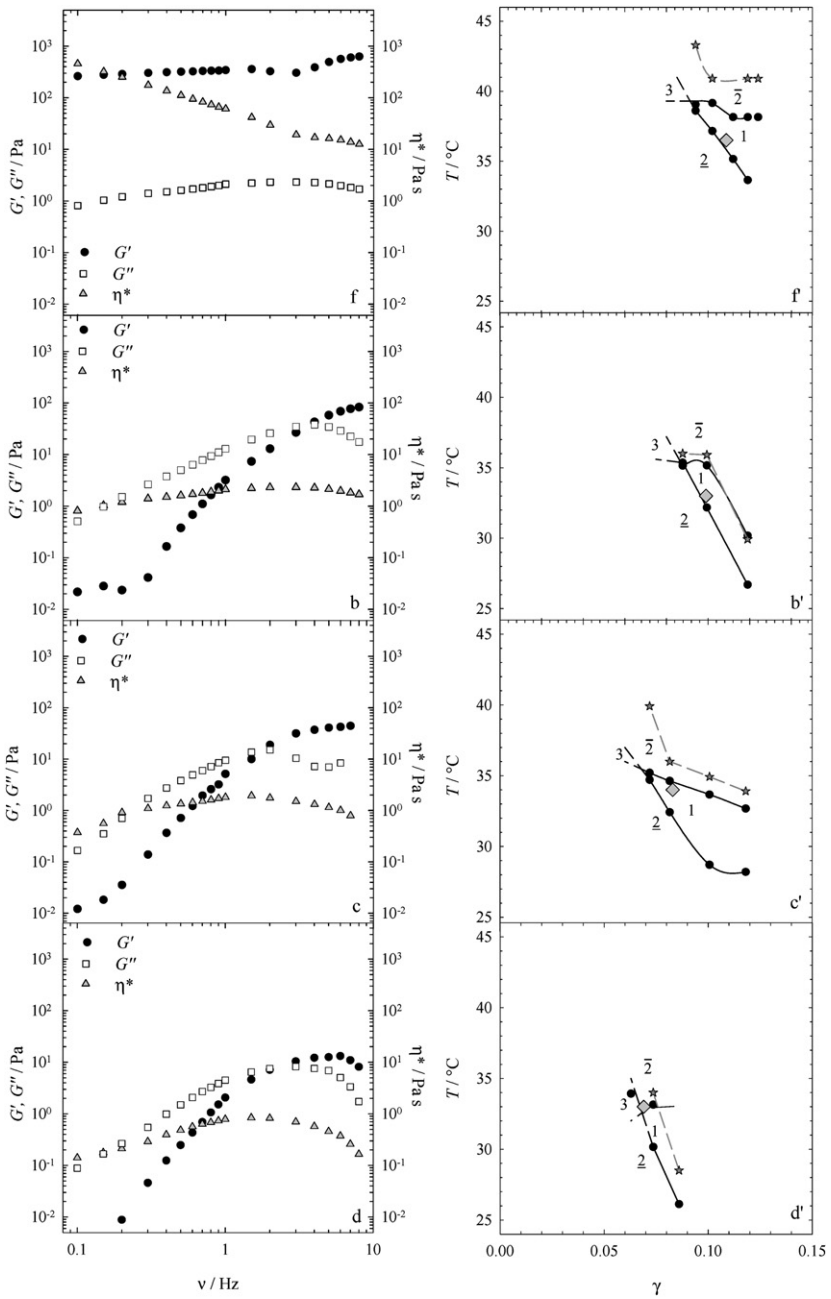

Fig. 5 Storage modulus G', loss modulus G'', and complex viscosity η^* as a function of the frequency ν (left) and phase diagrams (right) of the system H_2O/NIPAm/BisAm – *n*-dodecane/12-HOA – $C_{13/15}E_5$ at $\beta = 0.031$ and $\psi = 0.075$ measured for four different water-to-oil ratios α, namely $\alpha = 0.50$ (sample f), $\alpha = 0.34$ (sample b), $\alpha = 0.30$ (sample c), $\alpha = 0.25$ (sample d). The stars in the phase diagrams represent the sol–gel transition temperatures T_g and the diamonds the surfactant concentration γ and temperature T_{exp} of the samples used for the rheological measurements (see section 2.2.1 and Table 1). Note that for $\alpha = 0.30$ and $\alpha = 0.25$ LC phases are observed at $\gamma > 0.10$ and 0.08, respectively,[16] which are not indicated in the figures. Moreover, for $\alpha = 0.50$ only parts of the phase diagram are shown (see Fig. 4 for more details).

4.2. Influence of the water-to-oil ratio α

Considering the presence of the aqueous phase as "diluting" the network of the binary organogel automatically leads to the question of how the water-to-oil ratio influences the gel properties. According to the results of section 4.1 one expects that the gel gets the weaker the less oil is in the system. To prove or disprove this assumption we varied the water-to-oil ratio. Starting from equal amounts of water and oil ($\alpha = 0.5$) and a fixed gelator concentration in the oil phase of $\beta = 0.031$, we decreased the amount of the oil down to $\alpha = 0.25$. In a second set of measurements we combined the knowledge gained so far and tried to optimize the gel strength. For this purpose measurements at $\beta = 0.041$ and two different water-to-oil ratios were carried out.

4.2.1. α-Variation for β = 0.031. We first studied the influence of the water-to-oil ratio α on the viscoelastic properties of

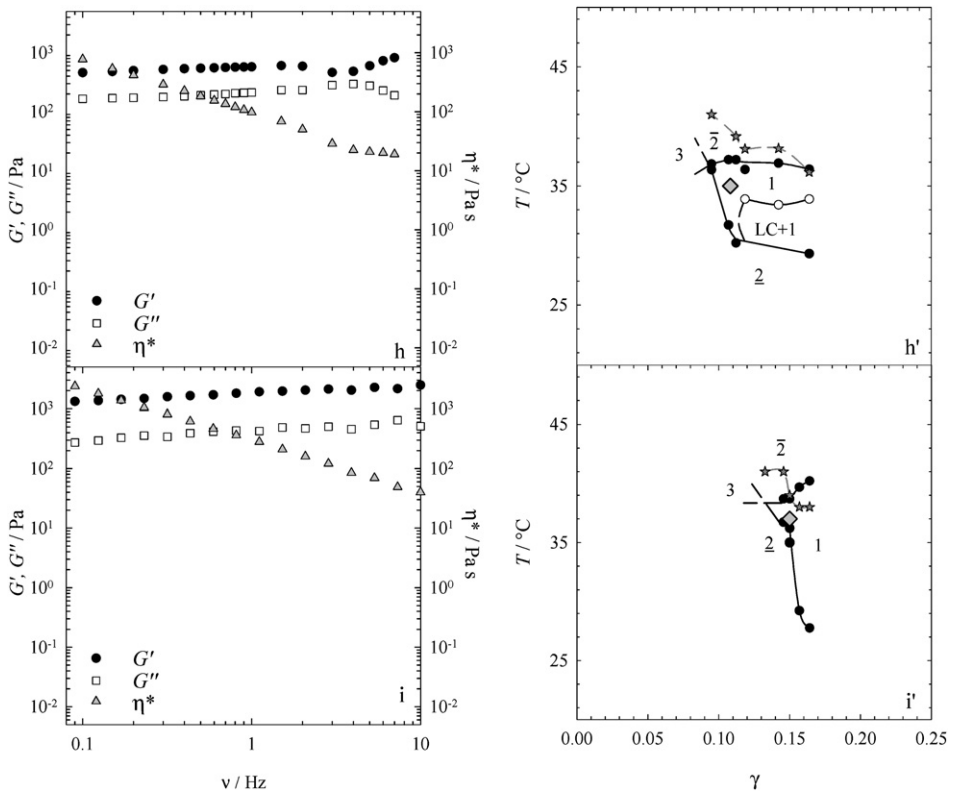

Fig. 6 Storage modulus G', loss modulus G'', and complex viscosity η^* as a function of the frequency ν (left) and phase diagrams (right) of the system H_2O/NIPAm/BisAm – *n*-dodecane/12-HOA – $C_{13/15}E_5$ at $\beta = 0.041$ and $\psi = 0.14$ measured for two different water-to-oil ratios α, namely $\alpha = 0.50$ (sample h), $\alpha = 0.60$ (sample i). The stars in the phase diagrams represent the sol–gel transition temperatures T_g and the diamonds the surfactant concentration γ and temperature T_{exp} of the samples used for the rheological measurements (see section 2.2.1 and Table 1).

the system H_2O/NIPAm/BisAm – *n*-dodecane/12-HOA – $C_{13/15}E_5$ at $\beta = 0.031$ and $\psi = 0.075$. In Fig. 5 the dynamic rheological data (left) and the phase diagrams (right) for four α values are shown.

Let us again first look at the phase diagrams. As can be seen in Fig. 5 (right) a decrease of α leads to a shift of the phase diagrams to lower temperatures and surfactant concentrations, which is always the case for non-ionic microemulsions.[1,14,15] What is remarkable is the fact that the sol–gel transition boundary also shifts to lower temperatures with decreasing α although the gelator concentration in the oil phase is kept constant. Moreover, the lower α the more difficult it was to gel the microemulsion. This macroscopic behavior is very nicely reflected in the rheological properties. Looking at Fig. 5 (left) one sees that a gel-like behavior is only observed at the highest α value (sample f). Note that the data are the same as those shown in Fig. 4 (middle). As already mentioned above three things are important to state for this sample: (a) both moduli are essentially frequency independent, *i.e.* the relaxation time of the system is extremely long, (b) the G'-values are of the order of 10^2 Pa and thus three orders of magnitude lower then the G'-values found for the binary system (10^5 Pa), (c) the G'-values are two orders of magnitude higher than the G''-values, which is typical for soft solids. The situation clearly changes if one decreases the amount of the oil phase. At lower α values, the system is a viscoelastic material with a finite relaxation time. In all cases ($\alpha = 0.34$, 0.30, and 0.25) a cross-over from liquid-like ($G'' > G'$) to solid-like ($G' > G''$) behavior is observed with increasing frequency. The relaxation time can be inferred from the frequency at which G' and G'' cross but, apparently, no significant α dependence is found and the relaxation times are similar to that observed for the system with $\alpha = 0.5$ and $\beta = 0.029$ (see Fig. 4). Coming back to Fig. 5 (left) one clearly sees that the behavior not only changes qualitatively for $\alpha \leq 0.34$ but also quantitatively, *i.e.* that both the G' and the G'' values decrease with decreasing α. The G' values of the sample with the lowest oil content ($\alpha = 0.25$) are only one order of magnitude higher than those of the non-gelled microemulsion (Fig. 3) and two orders of magnitude lower than those of the gelled microemulsion ($\alpha = 0.5$). In conclusion one can say that a gel-like behavior is only observed for $\alpha = 0.5$. All viscoelastic parameters decrease with decreasing α which can be explained by the fact that the volume of the gelled oil phase decreases with decreasing α. The larger the amount of the aqueous phase is, the smaller the effective amount of gelator, which, in turn, increases the distance between the cross-links and thus decreases the strength of the 3D network. At $\alpha = 0.5$ and $\beta = 0.031$ the gelator indeed is able to form a closely cross-linked permanent network, which transforms to a transient widely cross-linked network when diluted.

4.2.2. α-Variation for β = 0.041. The results presented so far clearly show that bicontinuous microemulsions can be gelled at gelator concentrations of $\beta \geq 0.031$ and a water-to-oil ratio of $\alpha = 0.5$. In order to find out whether it is possible to obtain a gel

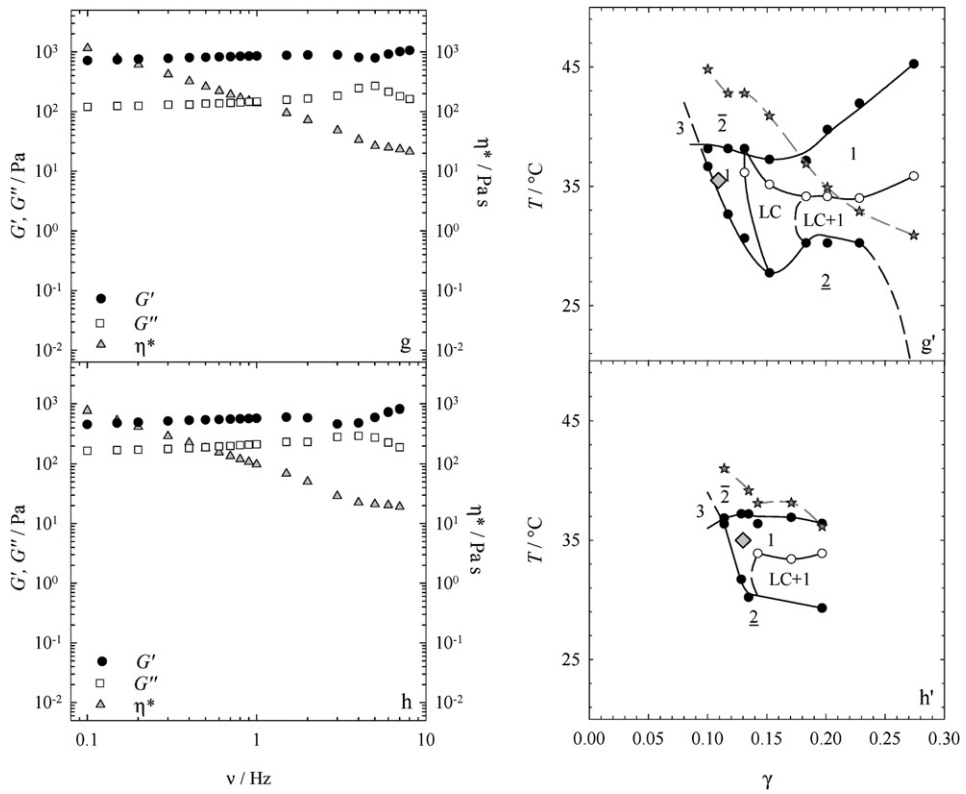

Fig. 7 Storage modulus G', loss modulus G'', and complex viscosity η^* as a function of the frequency ν (left) and phase diagrams (right) of the system H_2O/NIPAm/BisAm – *n*-dodecane/12-HOA – $C_{13/15}E_5$ at $\alpha = 0.5$ and $\beta = 0.041$ measured for two different monomer concentrations ψ, namely $\psi = 0.075$ (sample g) and $\psi = 0.14$ (sample h). The stars in the phase diagrams represent the sol–gel transition temperatures T_g and the diamonds the surfactant concentration γ and temperature T_{exp} of the samples used for the rheological measurements (see section 2.2.1 and Table 1). Data of phase diagram with $\psi = 0.075$ are adapted from ref. 2.

which is stronger than that of the system with $\beta = 0.041$ and $\alpha = 0.5$, the water-to-oil ratio α was increased from 0.5 to 0.6 at $\beta = 0.041$. Note that we also increased the monomer concentration ψ from 0.075 to 0.14 to compensate for the loss of NIPAm due to its surface activity.[16] However, the influence of the monomer concentration on the rheological properties is not very pronounced as will be shown below in section 4.3. Fig. 6 shows the dynamic rheological data (left) and the phase diagrams (right) of the system H_2O/NIPAm/BisAm – *n*-dodecane/12-HOA – $C_{13/15}E_5$ at two different α values.

The phase boundaries—including the sol–gel transition boundary—are shifted to higher temperatures with increasing α (Fig. 6 (right)). Again the increase of the sol–gel transition temperatures reflects the formation of a stronger gel, which is supported by the rheological data (Fig. 6 (left)). Both samples exhibit a gel-like behavior with both moduli being essentially frequency independent. The resulting G'-values are of the order of 10^3 Pa which is around two orders of magnitude lower then the G'-values found for the binary system (10^5 Pa). Another important result is the fact that indeed all rheological parameters (G', G'', η^*) increase with an increase of α following the same trend as observed for the α-variation at $\beta = 0.031$.

In conclusion one can say that the variation of the water-to-oil ratio α at a fixed gelator concentration β allows one to cover the whole spectrum of viscoelastic systems. The larger the amount of the oil phase the more gel-like the system. The fact that a bicontinuous microemulsion can be obtained at nearly any water-to-oil ratio[1,15] allows us to prepare bicontinuous gelled microemulsions with different water domain sizes. This feature will certainly play a role in our future work where we will polymerize the aqueous phase.

4.3. Influence of the monomer concentration ψ

Another important parameter that may have an influence on the gelation process of the bicontinuous microemulsion is the monomer concentration ψ of the aqueous phase. For optimizing the polymerization conditions it will be very important to play around with the monomer concentration and thus it is important to know whether or not the monomer concentration plays a role for the formation and the stability of the gel. To study the influence of the monomer concentration ψ on the viscoelastic properties of the microemulsion we took the system that forms the strongest gel and increased ψ from 0.075 to 0.138. The resulting rheological data and phase diagrams of the system H_2O/NIPAm/BisAm – *n*-dodecane/12-HOA – $C_{13/15}E_5$ measured at $\alpha = 0.5$, $\beta = 0.041$ and two different ψ values are presented in Fig. 7.

Looking at Fig. 7 two observations clearly indicate that increasing ψ weakens the gel. Firstly, the sol–gel transition boundary is shifted to lower temperatures (Fig. 7 (right)), while the position of the other phase boundaries is not affected

significantly. Secondly, the G' values of the system with $\psi = 0.075$ are about a factor 2 higher than those of the system with $\psi = 0.138$. However, compared to the influence of the gelator concentration β and the water-to-oil ratio α, respectively, the influence is small. Although an increase of ψ weakens the gel, one still observes a typical gel-like behavior and the slightly lower G' values could certainly be compensated for by a slight increase in β or α if need be. Note that the system has been chosen in such a way that the planned polymerization can be started *via* an intense UV light. Thus no polymers are expected to be formed during the rheological measurements or the phase studies. Actually, if polymer was formed higher G'-values would be observed for the system with the higher monomer concentration compared to the one with the lower monomer concentration, which was not observed.

5. Conclusions

The aim of the present study, which is the first of its kind, was to investigate the rheological behavior of gelled bicontinuous microemulsions. Our approach to gel the microemulsion was to add the gelator 12-hydroxyoctadecanoic acid (12-HOA) to the oil phase (*n*-dodecane) of the microemulsion. In order to understand how the presence of the non-gelled aqueous phase influences the properties of the organogel, the binary system 12-HOA – *n*-dodecane was studied first by "tabletop" and dynamic oscillatory experiments. The second step was to study the rheological properties of the respective polymerizable microemulsions, which consist of H_2O/NIPAm/BisAm – *n*-dodecane/12-HOA – $C_{13/15}E_5$ (NIPAm denotes the monomer *N*-isopropylacrylamide and BisAm the cross-linker *N*,*N*′-methylene bisacrylamide). The viscoelastic parameters were found to be strongly dependent on the composition of the system. An increase of the gelator concentration β and of the amount of the oil phase α induces a transition from a typical viscoelastic liquid to a viscoelastic gel. In the latter case the storage modulus G' and the loss modulus G'' are frequency independent and the G':G'' ratio was found to be 10:1 for the strongest gels. Comparing the G'-values of the gelled microemulsions with those of the binary organogel one sees that the former are 2–3 orders of magnitude lower. Obviously, the transition from a transient to a permanent gel network is induced if one increases β and α. The presence of the aqueous phase decreases the cross-link density and thus weakens the network. Another important result is the finding that the monomer concentration ψ also affects the strength of the gel. The larger ψ is, the weaker the gel. Finally it was found that the viscoelastic properties of the gelled microemulsion also depend on the type of oil and, not to be forgotten, on the temperature.

In conclusion one can say that we identified 5 different parameters which are important for the gelation of a bicontinuous microemulsion. The observed gel-like behavior of the microemulsions is caused by the gelled oil phase, which is most convincingly reflected in the destruction of the gel with decreasing gelator concentration and/or increasing water content. What could be learnt from the results obtained so far is that a minimum gelator concentration is required, that the mass fraction of the gelled oil phase should be as high as possible, that a high monomer concentration may destroy the gel and that the temperature should be kept as low as possible. Knowing how to prepare a strong and stable gelled bicontinuous microemulsion one can indeed use the microemulsion as template for the synthesis of high surface area polymers. The templating gel can easily be removed after the polymerization by simply raising the temperature above the sol–gel transition and washing the polymer with an appropriate solvent.

Acknowledgements

Financial support for this work was provided by the Marie Curie Research Training Network "Arrested Matter" (contract number MRTN-CT-2003-504712) and the Science Foundation Ireland (SFI-RFP07). B. M. thanks Fundação para a Ciência e tecnologia (FCT) (project ref. SFRH/BD/21467/2005).

References

1 T. Sottmann, R. Strey, in *Fundamentals of Interface and Colloidal Science*, ed. J. Lyklema, Elsevier, London, 2005, vol. 5, p. 5.1.
2 C. Stubenrauch, R. Tessendorf, R. Strey, I. Lynch and K. A. Dawson, *Langmuir*, 2007, **23**, 7730.
3 C. Stubenrauch, R. Tessendorf, A. Salvati, D. Topgaard, T. Sottmann, R. Strey and I. Lynch, *Langmuir*, 2008, **24**, 8473.
4 P. Terech, J. Barnes and G. B. McKenna, *Langmuir*, 1994, **10**, 3406.
5 *Techniques in the Life Sciences*, ed. E. R. Morris, S. B. Ross-Murphy, Elsevier, Amsterdam, 1981, vol. B3.
6 H. H. Winter, in *Encyclopedia of Polymer Science and Engineering*, ed. H. H. Mark, Wiley, New York, 1985, p. 343.
7 H. Rehage and H. Hoffmann, *Mol. Phys.*, 1991, **74**, 933.
8 P. Terech, D. Pasquier, V. Bordas and C. Rossat, *Langmuir*, 2000, **16**, 4485.
9 V. A. Mallia, M. George, D. L. Blair and R. G. Weiss, *Langmuir*, 2009, **25**, 8615.
10 P. Terech, C. Rossat and F. Volino, *J. Colloid Interface Sci.*, 2000, **227**, 363.
11 *Molecular Gels: Materials with Self-Assembled Fibrillar Networks*, P. Terech, R. G. Weiss, Springer, Dordrecht, 2006.
12 M. Gradzielski, H. Hoffmann, in *Handbook of Microemulsion Science and Technology*, ed. P. Kumar, K. L. Mittal, Marcel Dekker, New York, 1999, p. 357.
13 T. Sottmann, C. Stubenrauch, in *Microemulsions: Background, New Concepts, Appli- cations, Perspectives*, ed. C. Stubenrauch, Wiley-Blackwell, Oxford, 2009, (ch. 2).
14 M. Kahlweit, R. Strey, D. Haase, H. Kunieda, T. Schmeling, B. Faulhaber, M. Borkovec, H.-F. Eicke, G. Busse, F. Eggers, T. Funck, H. Richman, L. Magid, O. Södermann, P. Stilbs, J. Winkler, A. Dittrich and W. Jahn, *J. Colloid Interface Sci.*, 1987, **118**, 436.
15 S. Burauer, L. Belkoura, C. Stubenrauch and R. Strey, *Colloids Surf., A*, 2003, **228**, 159.
16 R. Tessendorf, Ph.D. Thesis, University of Cologne, 2009.

